

## ARTICLE

## Exploiting the labile site in dinuclear $[\text{Pd}_2\text{L}_2]^{n+}$ metallo-cycles: multi-step control over binding affinity without alteration of core host structure

Received 00th January 20xx,  
Accepted 00th January 20xx

DOI: 10.1039/x0xx00000x

James Kolien,<sup>a</sup> Amanda R. Inglis,<sup>a</sup> Roan A. S. Vasdev,<sup>b</sup> Ben I. Howard,<sup>a</sup> Paul E. Kruger,<sup>a</sup> Dan Preston,<sup>\*,a,c</sup>

While Nature often controls supramolecular processes through regulation giving multiple levels of activity, synthetic metallosupramolecular systems have generally been binary (e.g. on/off) when they have control over molecular recognition events, and have often relied upon drastic chemical transformations or complete disassembly to enforce this control. We report here a new low symmetry ligand with a bidentate and a monodentate site (L). In combination with  $\text{Pd}^{2+}$ , this ligand forms a [2 + 2] metallo-macrocyclic,  $[\text{Pd}_2\text{L}_2\text{L}'_2]^{n+}$ , where L' is the monodentate ancillary ligand that occupies the fourth and final coordination site of the metal ions. This assembly is structurally simple, but displays nuanced, multi-step binding affinity toward a neutral diplatinate guest employed for proof-of-concept. This complexity is introduced through varying the identity of L', which can either be solvent (DMSO) or the halides chloride, bromide or iodide. The identity of L' alters the cationic charge of the complex (neutral DMSO versus monoanionic halides) or otherwise influences the electron deficiency of the binding site of the host through varied strength of halide-ligand intra-molecular hydrogen bonding. Cycling between these different complexes was demonstrated, except for L' = chloride which is non-reversible. This system therefore is able to interact with a platinate guest with four different graduations of affinity in response to stimuli, while still retaining the same simple core cationic structure. In addition to multi-setting binding affinity, we believe this is the first example of the use of variable intramolecular hydrogen bonding strength in switchable ancillary ligands to alter the electronic character and hence the  $\pi$ - $\pi$  recognition characteristics of a metallosupramolecular host.

### Introduction

Supramolecular chemistry is the tool that Nature uses to drive its machinery. It enables the recognition processes that facilitate molecular replication and transcription,<sup>[1]</sup> molecular storage<sup>[2]</sup> and transport,<sup>[3]</sup> movement, and encapsulation/binding events that allow chemical transformations of substrates by enzymatic proteins.<sup>[4]</sup> A key characteristic of these processes is that they can be regulated. This regulation is often not simply binary (on/off) but has multiple settings of activity level.<sup>[5]</sup> Additionally, interchange between these levels can be achieved through alterations of the electronic character or conformation of the biological machinery, rather than by simply influencing translation or degradation.<sup>[5-6]</sup> These alterations can be reversibly enacted

through small-molecule binding, phosphorylation, or protein-protein interactions.<sup>[6a, 7]</sup>

Metallosupramolecular chemists are intensely interested in molecular recognition,<sup>[8]</sup> using self-assembled hosts to bind guests for a diverse set of applications including molecular storage of reactive species,<sup>[9]</sup> environmental pollutants<sup>[10]</sup> and chemical warfare agent analogues,<sup>[11]</sup> for drug delivery<sup>[12]</sup> and biological diagnostics,<sup>[13]</sup> and catalysis<sup>[14]</sup> and chemical transformations carried out in confined spaces.<sup>[15]</sup> Ideally, these processes should also be capable of being regulated.<sup>[16]</sup> A wide variety of stimuli have been employed towards the host<sup>[17]</sup> to regulate activity, including light,<sup>[18]</sup> acid/base<sup>[12c]</sup> and redox<sup>[19]</sup> chemistry, transmetalation,<sup>[20]</sup> stoichiometry,<sup>[21]</sup> and ancillary ligand identity.<sup>[22]</sup> In contrast to biological systems, these synthetic analogues generally have two characteristics: 1) regulation is binary (on/off or sometimes high/low activity), and 2) regulation is most often achieved through significant structural transformation of the host architecture; generally a partial<sup>[21-22]</sup> or complete<sup>[12c, 18-19, 23]</sup> disassembly of the host structure.

In some cases, activity has been regulated (in a binary fashion) while retaining core connectivity. The Fujita group has reported a  $[\text{Pd}_{12}\text{L}_{24}]^{24+}$  system with internally directed azo-benzene units capable of light/heat driven isomerism.<sup>[24]</sup> The *trans* isomer

<sup>a</sup>MacDiarmid Institute for Advanced Materials and Nanotechnology, School of Physical and Chemical Sciences, University of Canterbury, Christchurch 8041, New Zealand.

<sup>b</sup>Department of Chemistry, University of Otago, PO Box 56, Dunedin 9054, New Zealand.

<sup>c</sup>Research School of Chemistry, The Australian National University, Canberra, ACT 2600, Australia. E-mail: Daniel.Preston@anu.edu.au

Electronic Supplementary Information (ESI) available: <sup>1</sup>H, <sup>13</sup>C, and 2D NMR data, HR-ESI-MS spectra, computational information and modelling data. For ESI and structural data in xyz or other electronic format see DOI:10.1039/x0xx00000x

interacted with 1-pyrenecarboxaldehyde, while the *cis* isomer did not. Light has also been used by Clever and co-workers in a  $[\text{Pd}_2\text{L}_4]^{4+}$  cage with ligands capable of photo-driven cyclisation to influence binding affinity for a  $\text{B}_{12}\text{F}_{12}^{2-}$  guest.<sup>[17b]</sup> There have also been examples involving much more subtle changes. Yam and co-workers used alteration of pH with a macrocyclic  $[\text{Pt}_2\text{LL}']$  system containing a protonatable pyridyl nitrogen in the cavity,<sup>[25]</sup> using steric and electronic repulsion to reversibly eject a neutral palatinite guest. Sallé and co-workers have also used redox chemistry with a platinum(II) cage with tetrathiafulvalene-based ligands to alter affinity of the cage towards coronene in the presence of a competing anionic guest, whilst retaining core structure.<sup>[17d]</sup> Very recently, Akine and co-workers have used a *bis*-cobalt(II) complex formed with a macrocyclic ligand, and have (non-reversibly) exchanged the axial ligands at the metal centres to alter the charge of the complex and hence its affinity for sodium cations.<sup>[26]</sup>

The majority of metallosupramolecular assemblies have been constructed with the reliable square planar metal ions, hemilabile palladium(II) and inert platinum(II). Synthetic strategies have been developed to access different structural types, defined largely by the arrangement and denticity of the ligands around the metal ions (Figure 1).<sup>[27]</sup>

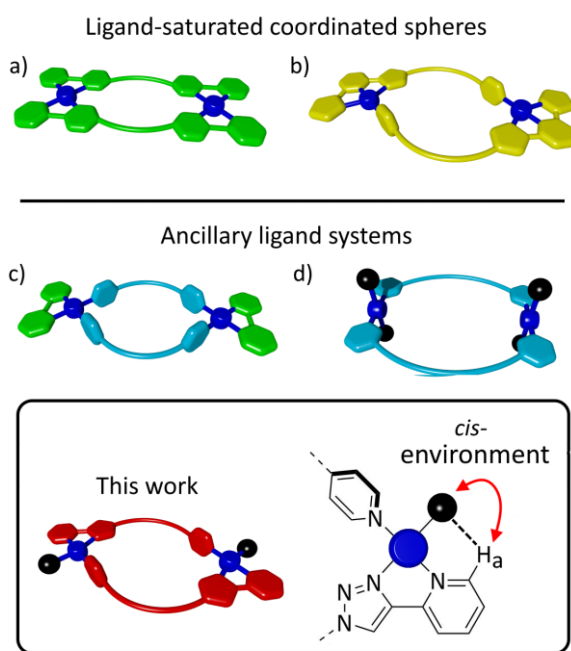


**Figure 1** The coordination spheres of metal ions in various types of metallosupramolecular assemblies (shown for dinuclear assemblies, but also applicable to many systems of higher nuclearity). Assemblies with spheres saturated by structurally linking ligands: a) metal centres with bidentate linking ligands, and b) metal centres with monodentate and tridentate linking ligands. Assemblies with ancillary ligands: c) metal centres with *cis*-capped bidentate ancillary ligands with monodentate linking ligands, or d) two monodentate ancillary ligands at each metal centre. *Bottom*: the system with a single monodentate ancillary ligand at each metal ion employed in this work. This system holds the bidentate site in the plane of the ancillary ligand, with the *ortho* proton of the pyridyl ring *cis* to this ligand directed towards it (see figure), and thus readily influenced if the ancillary ligand is a hydrogen-bonding acceptor.

Two of these arrangements always result in the formation of metallo-cyclic (or sometimes cage) structures in which the coordination spheres of the metal ions are exclusively occupied

by core ligands linking the structure together. These contain either a) metal ions linked into assemblies *via* bidentate ligands<sup>[28]</sup> (Figure 1a), or b) metal ions linked into assemblies with a complementary combination of monodentate and tridentate sites on ligands<sup>[25, 29]</sup> (Figure 1b). A characteristic of these two assembly types is that methodologies for the reversible exchange of these ligands have not yet been well developed.

There are also systems in which the coordination sphere of the metal ion is occupied by a combination of monodentate linking ligands and ancillary capping ligands. In one of these, *cis*-capped metal ions are linked into a larger unified structure with monodentate ligands, in work from the groups of Fujita, Chand, Peinador, Peris and others (Figure 1c).<sup>[30]</sup> While Chand and co-workers have explored the replacement of ancillary capping groups<sup>[31]</sup> in systems of type, the reversible exchange of ligands in these systems has not been achieved.

Assemblies with metal ions surrounded by four monodentate donors have generally seen these donors all being part of core linking ligands (*i.e.* cages).<sup>[32]</sup> But strongly donating and bulky phosphines have also been used to enforce *trans* geometry of linking ligands at the metal centre, often with acetylide ligands.<sup>[33]</sup> There have also been examples from Raymond and co-workers,<sup>[34]</sup> Hiraoka, Sakata and Shionoya,<sup>[35]</sup> Puddephat and co-workers,<sup>[36]</sup> Crowley and co-workers<sup>[22a, 37]</sup> Clever and co-workers,<sup>[38]</sup> and Hanan and co-workers<sup>[39]</sup> in which *trans* sites at the metal ion are occupied by halides (Figure 1d).<sup>[40]</sup> In the case of the example from Crowley and co-workers, a  $[\text{Pd}_2\text{L}_2\text{Cl}_2]$  macrocycle could be reversibly transformed into a  $[\text{Pd}_2\text{L}_4]^{4+}$  cage by addition of  $\text{Ag}^+$  or  $\text{Cl}^-$ , with the neutral macrocycle not binding *exo*- or *endo*-bound guests.<sup>[22a]</sup>

In our work on metallosupramolecular chemistry,<sup>[41]</sup> we have an interest in using stimuli to effect structural transformations.<sup>[28c, 29e, 42]</sup> As part of our efforts we recently reported a simple ligand, with both a bidentate 2-pyridyl-1,2,3-triazole chelator and a monodentate pyridyl donor. When combined with  $\text{Pd}^{2+}$  in a 2:2 ratio, a simple  $[\text{Pd}_2\text{L}_2(\text{solvent})_2]^{4+}$  macrocycle was formed. Each metal ion had a coordination sphere filled with the bidentate site from one ligand, the monodentate site from the other, with the final site occupied with an ancillary ligand which was in this case ligated solvent (acetonitrile or DMSO) (Figure 2 *top*). We noticed two key characteristics of this new assembly type. Firstly, unlike bidentate capping units (Figure 1c), the ancillary ligand played no key structural role, and was in effect solely present to complete the coordination sphere of the metal ion. This suggested that it could be readily (and potentially reversibly) exchanged without disruption of the core cationic structure. Secondly, and unlike systems with two monodentate ancillary ligands and monodentate linking ligands (Figure 1d), as the bidentate site was in the same plane as the ancillary ligand, the proton *ortho* to the nitrogen atom of the pyridine from the bidentate site was directed and held fixed in position in this plane towards the ancillary ligand. This led us to hypothesise that this hydrogen atom, and therefore the bidentate site,

would be highly sensitive to the identity and influence of the ancillary ligand, say (for example) through hydrogen bonding (Figure 1 *bottom right*).

With this in mind, this first generation structure encouraged us to here create an analogue and explore the effects of alteration of the ancillary ligand. We were particularly interested in using the identity of the ancillary ligand to influence another field in which we are interested, molecular recognition.<sup>[14b, 43]</sup> We report here a new ligand, with a 2-pyridyl-1,2,3-triazole bidentate chelator which has a 1,3-substituted phenyl corner, a 4-(phenyl)pyridine arm, and is solubilised with a methyltriglycol chain (L, Figure 2 *bottom*). In 2:2 combination with Pd<sup>2+</sup> and the appropriate halide source when required, we are able to access [Pd<sub>2</sub>L<sub>2</sub>L'<sub>2</sub>]<sup>n+</sup> macrocycles, where L' = solvent (n = 4) or the halides Cl<sup>-</sup>, Br<sup>-</sup> or I<sup>-</sup> (n = 2) (Figure 2 *bottom*). Except for L' = Cl<sup>-</sup>, the identity of L' is interchangeable. Each complex interacts with a neutral diplatinate guest, with altered affinity in each case.

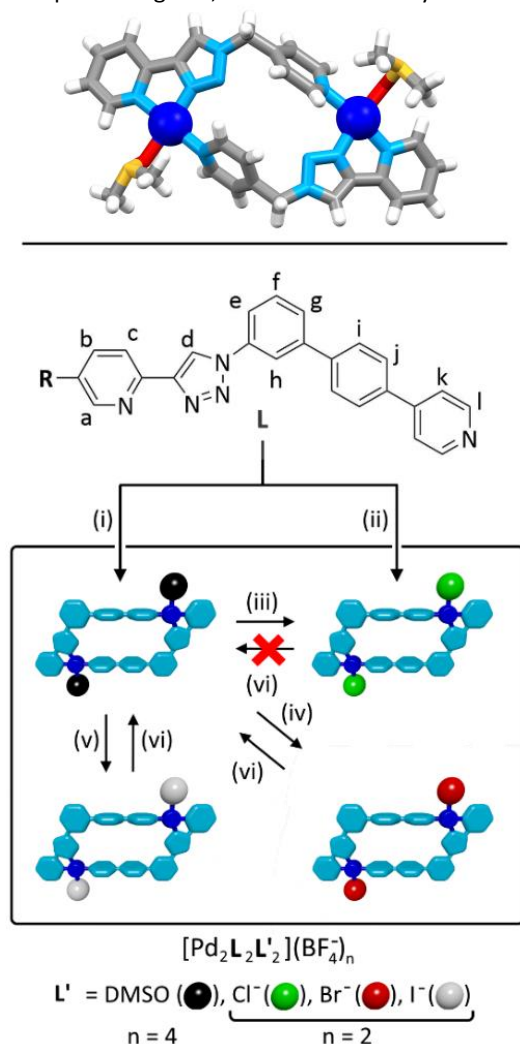


**Figure 2** Above: the previously reported<sup>[42b]</sup> [Pd<sub>2</sub>L<sub>2</sub>(solvent)<sub>2</sub>]<sup>4+</sup> complex, colours: carbon grey, hydrogen white, nitrogen light blue, oxygen red, palladium dark blue, sulphur yellow; Below: The ligand L (R = methyltriglycol and its conversion into [Pd<sub>2</sub>L<sub>2</sub>L'<sub>2</sub>]<sup>n+</sup> complexes. Conditions: (i) [Pd(CH<sub>3</sub>CN)<sub>4</sub>](BF<sub>4</sub>)<sub>2</sub>, [D<sub>3</sub>]acetonitrile or [D<sub>6</sub>]DMSO, (ii) [Pd(CH<sub>3</sub>CN)<sub>2</sub>Cl<sub>2</sub>], AgBF<sub>4</sub>, [D<sub>3</sub>]acetonitrile or [D<sub>6</sub>]DMSO. *In situ* conversion carried out in [D<sub>6</sub>]DMSO, (iii) tetraethylammonium chloride, (iv) tetraethylammonium bromide, (v) potassium iodide, (vi) AgBF<sub>4</sub>.

This affinity is driven by the charge on the complex, or the varied strength of hydrogen bonding between halide and the *ortho* proton of the pyridyl ring from the bidentate site. This is therefore a system where, highly unusually, variation of the ancillary ligand gives several different complexes sharing the same core structure but allows multiple-setting graduated control over binding affinity for molecular recognition.

## Results and Discussion

### Synthesis

The ligand L (Figure 2) was synthesised in four steps (ESI<sup>†</sup> S2.2 to 2.5, yield at final step 89%). It was characterised with a suite of techniques including NMR spectroscopies, and mass spectrometry (m/z = 538.2466, [MH]<sup>+</sup>, ESI<sup>†</sup> S2.5).

Combination of L with [Pd(CH<sub>3</sub>CN)<sub>4</sub>](BF<sub>4</sub>)<sub>4</sub> in [D<sub>3</sub>]acetonitrile or [D<sub>6</sub>]DMSO in a 2:2 ratio at [L] ≤ 5 mM (2.5 mM for the complex, see below) resulted in a single set of ligand environments in the <sup>1</sup>H NMR spectra, indicating formation of a single, highly symmetrical structure (Figure 2, Figure 3b).

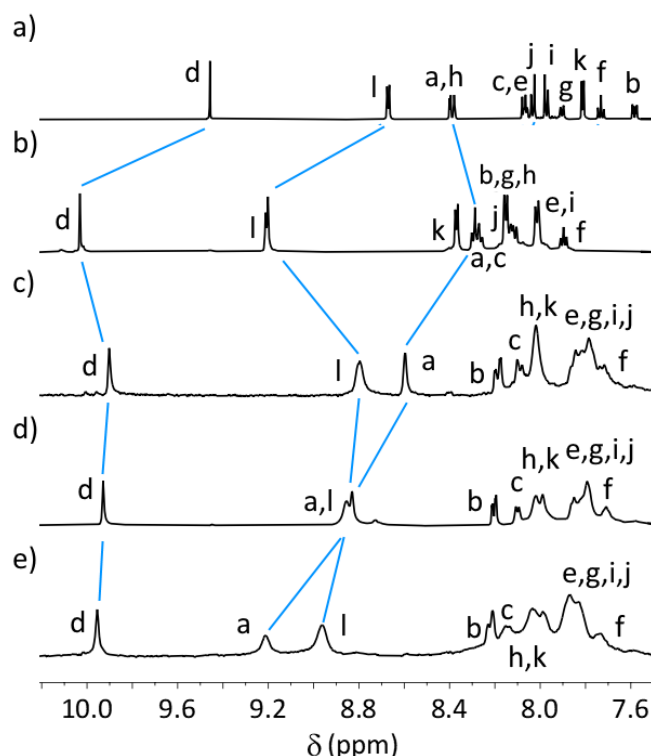


**Figure 3** Partial stacked <sup>1</sup>H NMR spectra (600 MHz, [D<sub>6</sub>]DMSO, 298 K) of a) L, b) [Pd<sub>2</sub>L<sub>2</sub>(solvent)<sub>2</sub>](BF<sub>4</sub>)<sub>4</sub>, c) [Pd<sub>2</sub>L<sub>2</sub>Cl<sub>2</sub>](BF<sub>4</sub>)<sub>2</sub> and d) [Pd<sub>2</sub>L<sub>2</sub>Br<sub>2</sub>](BF<sub>4</sub>)<sub>2</sub>, and e) [Pd<sub>2</sub>L<sub>2</sub>I<sub>2</sub>](BF<sub>4</sub>)<sub>2</sub>. Differences in chemical shift for key resonances highlighted with the use of blue lines. All spectra obtained at [L] = 5 mM ([complex] = 2.5 mM).

This spectral transformation was instantaneous in [D<sub>6</sub>]DMSO, but required heating at 40 °C for four hours in [D<sub>3</sub>]acetonitrile. These peaks were at higher chemical shift than that of the free ligand, in particular for peaks associated with the 2-pyridyl-1,2,3-triazole bidentate pocket (in [D<sub>6</sub>]DMSO Δδ(H<sub>b</sub>) = ~ 0.6 ppm, Δδ(H<sub>d</sub>) = 0.58 ppm), and the monopyridyl arm, Δδ(H<sub>l</sub>) = 0.56 ppm.

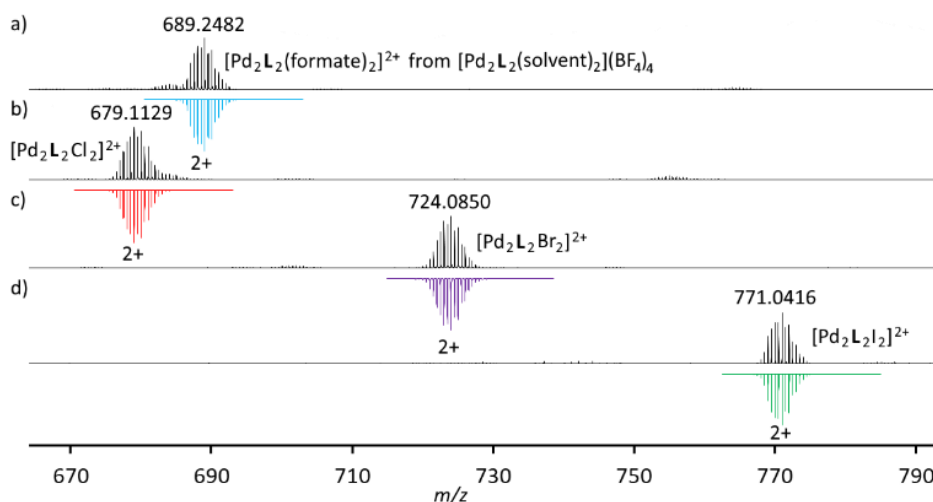


**Figure 4** Partial mass spectra (DMSO/DMF) for  $[\text{Pd}_2\text{L}_2\text{L}'_2]^{n+}$ , where  $\text{L}' = \text{a) solvent, b) Cl, c) Br, and d) I}$ . Observed spectra shown in black, calculated spectra shown below and inverted in colour. Formate in (a) generated from formic acid in mass spectral conditions.

This indicated metal ion coordination at these sites. The lack of a large downfield shift for proton resonance  $\text{H}_a$  indicated that the bidentate pockets were not arranged in a head-to-tail arrangement at a metal centre,<sup>[44]</sup> and that  $\text{H}_a$  was not participating in a significant hydrogen bond, and was a characteristic of the previously reported  $[\text{Pd}_2\text{L}_2(\text{solvent})_2]^{4+}$  complex in both DMSO and acetonitrile.<sup>[42b]</sup>

High resolution electrospray ionisation mass spectrometry (HR ESI-MS) of these samples confirmed formation of a  $[2 + 2]$  complex (Figure 4a and  $\text{ESI}^+$ , for example,  $m/z = 444.4970$   $[\text{Pd}_2\text{L}_2 + \text{HCOO}]^{3+}$  and  $689.2482$   $[\text{Pd}_2\text{L}_2 + 2\text{HCOO}]^{2+}$ , formate originating from formic acid in mass spectral conditions). In a  $[2 + 2]$  complex with a symmetrical NMR spectrum, only a single structural configuration is possible, and must be analogous to the crystal structure from our previous work<sup>[42b]</sup>: with each of the two  $\text{Pd}^{2+}$  metal ions coordinated to the 2-pyridyl-1,2,3-triazole site of one ligand, the monopyridyl arm of the other ligand, with the remaining site (*trans* to the coordinated N3 nitrogen of the triazole ring) occupied by solvent.

No solvent was observed in the identified species via mass spectrometry, but this weak coordination bond was presumably fragmented under MS conditions.  $^{19}\text{F}$  NMR spectroscopy of the complex with comparison to  $[\text{N}(\text{CH}_3)_4]\text{BF}_4$  confirmed that the  $\text{BF}_4^-$  counterions were not coordinated at the final site in solution ( $\text{ESI}^+$ , Figure S2.19). With DMSO ligated, coordination to  $\text{Pd}^{2+}$  has been repeatedly reported crystallographically through both the sulphur<sup>[45]</sup> and oxygen<sup>[46]</sup> donors. While attempts to crystallise the  $[\text{Pd}_2\text{L}_2(\text{solvent})_2](\text{BF}_4)_4$  product were unsuccessful from either DMSO or acetonitrile, DFT optimised structures (BP86/def2-SVP) showed that the proposed  $[2 + 2]$  structure was feasible (Figure 5a). They also indicated that the *O*-bound complex was highly favoured (by  $55 \text{ kJ mol}^{-1}$ ,  $\text{ESI}^+$ ) over the *S*-bound complex. In light of this, it is likely that here the ligand is under fast exchange conditions, favouring the *O*-bound

binding mode in the time-averaged NMR spectrum. This is the same coordination mode observed in the crystal structure of the original analogue (Figure 2 top). The product was isolated through precipitation from acetonitrile with diethyl ether (87%). At concentrations above 2.5 mM for the complex, the  $^1\text{H}$  NMR spectra became untidy and broad, indicating formation of oligomers and larger macrocycles ( $\text{ESI}^+$ , Figure S2.15).<sup>[47]</sup> Despite the solubilising poly(ethyleneglycol) chains, in acetonitrile these mixtures precipitated or underwent gelation over several days. At  $\leq 5 \text{ mM}$  in acetonitrile, precipitation still occurred, but at a reduced rate. Solutions were stable in DMSO.

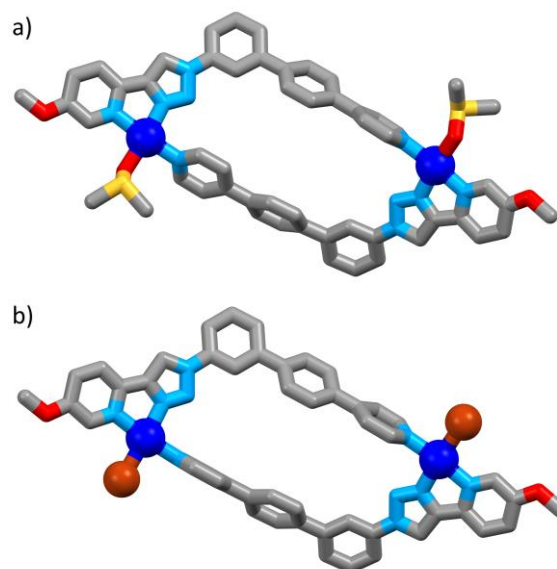


**Figure 5** DFT optimised structures (BP86/def2-SVP) depicting a)  $[\text{Pd}_2\text{L}_2(\text{DMSO})_2]^{4+}$  and b)  $[\text{Pd}_2\text{L}_2\text{Br}_2]^{2+}$  in tube form. The structure in a) was calculated with the DMSO *O*-bound, which was lower in energy to *S*-bound. Methyltriglycol chains were curtailed to methoxy groups for computational simplicity. Hydrogen atoms omitted for clarity. Colors: carbon grey, hydrogen white, bromine brown, nitrogen blue, oxygen red, palladium dark blue, sulphur yellow.

We next synthesised the dicationic complex with solvent molecules replaced with anionic ligands,  $[\text{Pd}_2\text{L}_2\text{Cl}_2](\text{BF}_4)_2$ . This was accessed through combination of a 2:2 ratio of  $[\text{Pd}(\text{CH}_3\text{CN})_2\text{Cl}_2]$  and  $\text{AgBF}_4$  in  $[\text{D}_3]\text{acetonitrile}$ , followed by removal of the  $\text{AgCl}$  precipitate through centrifugation and addition of 2 equivalents of  $\text{L}$  (Figure 2 below). Precipitation with diethyl ether rendered the compound as a white solid (yield 83%,  $\text{ESI}^+$  S2.8). Similar results were obtained in DMSO.



The solubility properties of this complex were similar to those of tetracationic complex. With molecular identity confirmed (see below) we next set out to ensure that we could access  $[\text{Pd}_2\text{L}_2\text{X}_2]^{2+}$  metallocycles in solution through *in situ* generation from a 1:2 combination<sup>[48]</sup> of  $[\text{Pd}_2\text{L}_2(\text{DMSO})_2]^{4+}$  and the appropriate halide source (tetraethylammonium chloride/bromide, or potassium iodide) (Figure 2 *bottom*).

The predominant peak in the mass spectra of all these samples was that corresponding to  $[\text{Pd}_2\text{L}_2\text{X}_2]^{2+}$  (Figure 4b – d, for example, for  $[\text{Pd}_2\text{L}_2\text{Cl}_2]^{2+}$   $m/z = 679.1129$ ). Again, DFT calculations (BP86/def2-SVP, for  $\text{L}' = \text{Br}$ , Figure 5b) showed that the formation of these complexes with the same core structure as with  $\text{L}' = \text{DMSO}$  was feasible.

The  $^1\text{H}$  NMR spectra ( $[\text{D}_6]\text{DMSO}$ ) of the dicationic complexes (Figure 3c – e) showed a single set of resonances, consistent with the formation of single high-symmetry products. The resonances proximal to coordination sites were shifted downfield from that of the free ligand (Figure 3a) but upfield (in most cases but with  $\text{H}_a$  as a notable exception, see below) with respect to  $[\text{Pd}_2\text{L}_2(\text{DMSO})_2]^{4+}$ , consistent with the formation of a coordination complex with lower cationic charge. There were two important spectral trends for the halide complexes. The first of these was an increasing broadening of the spectral peaks (in comparison to  $[\text{Pd}_2\text{L}_2(\text{DMSO})_2]^{4+}$ ) going from  $\text{Cl}^-$  to  $\text{I}^-$ . We considered two possible rationales for this: 1) hindered rotation of the phenyl pyridyl arms by the bulky halide ligands, or 2) ligand fluxionality on the  $^1\text{H}$  NMR timescale. Collection of  $^1\text{H}$  NMR spectra at elevated temperatures resulted in sharpening of most peaks in the spectra: the spectra were sharp at 50 °C for  $\text{L}' = \text{Cl}^-$  and  $\text{Br}^-$ , but broad for iodide but for  $\text{L}' = \text{I}^-$  heating to 100 °C was required to remove the broadness of the peaks (ESI† Figures S2.30 to S2.32).

Conversely, the  $\text{H}_a$  resonance broadened very slightly upon heating for  $\text{L}' = \text{Cl}^-$  and  $\text{Br}^-$ , but for  $\text{L}' = \text{I}^-$ , the  $\text{H}_a$  peak became very broad (ESI†, Figures S2.30 to S2.32). We ascribe this to the processes 1) and 2) above. It would be expected that rotation of the (phenyl)pyridyl arm would be slower with increasing ionic radius of the halide, hence the higher temperatures required to sharpen the peaks for  $\text{L}' = \text{I}^-$  as opposed to  $\text{Cl}^-$  or  $\text{Br}^-$ . Secondly, the effects of ligand fluxionality should be experienced to a greater extent by  $\text{H}_a$  than other proton resonances (see the discussion on hydrogen bonding below). The broadening of the  $\text{H}_a$  resonance for  $\text{I}^-$  is consistent with this halide being more labile than the others.

To confirm the relative ordering of halide lability, we generated equilibrium mixtures containing 1 equivalent of  $[\text{Pd}_2\text{L}_2(\text{solvent})_2]^{4+}$  and 1 equivalent of each halide. These could also be formed from equimolar combination of  $[\text{Pd}_2\text{L}_2(\text{solvent})_2]^{4+}$  and  $[\text{Pd}_2\text{L}_2\text{X}_2]^{2+}$ . Equilibration for  $\text{Br}^-$  and  $\text{I}^-$  occurred in the time taken to run the NMR sample, for  $\text{Cl}^-$  20 minutes was required (RT). At 50 °C the chloride-containing mixture contained several species (Figure 6b). Two of these

were readily identifiable as  $[\text{Pd}_2\text{L}_2(\text{solvent})_2]^{4+}$  and  $[\text{Pd}_2\text{L}_2\text{Cl}_2]^{2+}$  (see Figure 6a and c).

While there was overlap in some regions, additional  $\text{H}_a$  and  $\text{H}_i$  environments could be observed that were consistent with a second, different chloride-ligated metal centre. Integration suggested that there was also a second solvent-ligated metal centre (for example, it was consistent with two coincident  $\text{H}_i$  resonances of this nature), suggesting a third species that was  $[\text{Pd}_2\text{L}_2(\text{solvent})\text{Cl}]^{3+}$ , consistent with the stoichiometry of the system. A 3+ peak corresponding to  $[\text{Pd}_2\text{L}_2\text{Cl}]^{3+}$  was observed in the mass spectrum of this mixture (ESI†, Figure S2.34): the equivalent peak had not previously been observed in the sample containing solely the dichloride complex.

Hence, the solution contained separate and stable species at 50 °C (Figure 6b). Heating to 100 °C did not merge the peaks associated with chloride- and solvent-ligated centres (ESI† Figure S2.33). With iodide, at 50 °C the solution contained a single (broad) set of resonances with the  $\text{H}_a$  resonance broadened into the baseline (Figure 6e). These resonances were at intermediate chemical shifts to those of pure  $[\text{Pd}_2\text{L}_2(\text{solvent})_2]^{4+}$  and  $[\text{Pd}_2\text{L}_2\text{I}_2]^{2+}$  at the same temperature (Figure 6 d and f). The spectra sharpened further upon heating to 100 °C (ESI†, Figure S2.36). The behaviour with bromide was intermediate between the other two halides, but closer to that of chloride (ESI†, Figure S2.35). Therefore, the lability of the halide ligands was ordered  $\text{Cl}^- < \text{Br}^- < \text{I}^-$ .

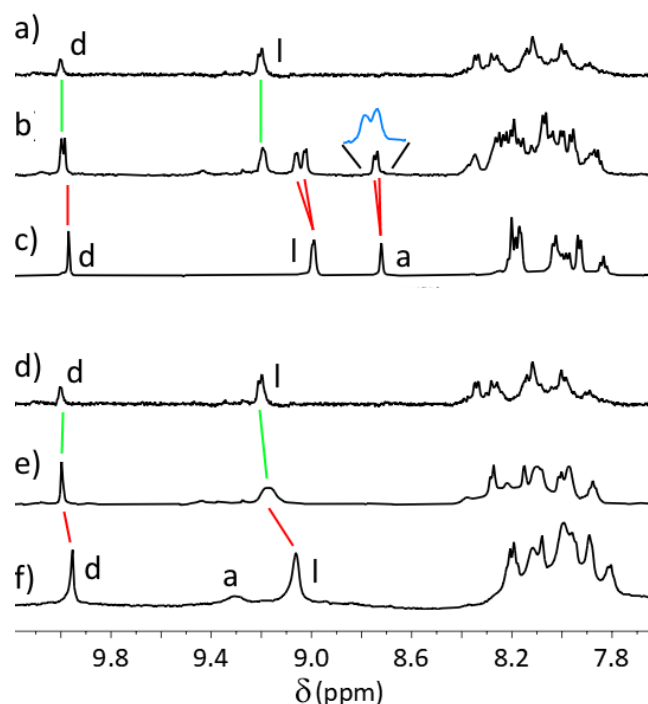


**Figure 6** Partial  $^1\text{H}$  NMR spectra (600 MHz,  $[\text{D}_6]\text{DMSO}$ , 323 K) of a)  $[\text{Pd}_2\text{L}_2(\text{DMSO})_2]^{4+}$ , b) 1:1  $[\text{Pd}_2\text{L}_2(\text{DMSO})_2]^{4+}$  and  $[\text{Pd}_2\text{L}_2\text{Cl}_2]^{2+}$ , c)  $[\text{Pd}_2\text{L}_2\text{Cl}_2]^{2+}$ , d)  $[\text{Pd}_2\text{L}_2(\text{DMSO})_2]^{4+}$ , e) 1:1  $[\text{Pd}_2\text{L}_2(\text{DMSO})_2]^{4+}$  and  $[\text{Pd}_2\text{L}_2\text{I}_2]^{2+}$ , and f)  $[\text{Pd}_2\text{L}_2\text{I}_2]^{2+}$ . Spectra are presented at 323 K because for mixed spectra (b and e) these were untidy at 298 K (ESI†, Figure S2.33).

The second trend of note within the  $^1\text{H}$  NMR spectra at 298 K (Figure 3) was the chemical shifts of the proton resonance  $\text{H}_a$ . These were shifted downfield from both free ligand and the  $[\text{Pd}_2\text{L}_2(\text{DMSO})_2]^{4+}$  complex: compared to free ligand,  $\text{L}' = \text{Cl}^-$   $\Delta\delta(\text{H}_a) = 0.21$  ppm,  $\text{Br}^-$   $\Delta\delta(\text{H}_a) = 0.47$  ppm, and  $\text{I}^-$   $\Delta\delta(\text{H}_a) = 0.86$  ppm. This represents considerable alteration of the electronic environment of  $\text{H}_a$ . These shifts, localised close to the *cis*-environment from the halide, are far greater than the differences for other environments. These other resonances are close to equivalent in terms of chemical shift across the halide series, although follow the same trend across the halides as  $\text{H}_a$ .

While the identity of the halide will obviously influence the whole of the metal-coordinating environment, we do not believe that the donor strength of the individual halides satisfactorily explains the significant alteration in chemical shift of the  $\text{H}_a$  proton. Interactions of either  $\sigma$ - or  $\pi$ -donor type will be manifested primarily in alteration of chemical shifts proximal to the *trans* position from the ancillary ligand, namely the triazole proton ( $\text{H}_a$ ). As previously mentioned, the  $\text{H}_a$  resonance is sensitive to hydrogen bonding effects.<sup>[28c, 42b, 44]</sup> We therefore attribute the change in chemical shift for  $\text{H}_a$  across the ancillary ligands to hydrogen bonding between the halide as acceptor and the acidic C-H as donor. This hydrogen bond is evident in all three DFT-calculated structures (D-H...A angles from  $123^\circ$  to  $127^\circ$ , H...A distances from 2.555 to 2.827 Å) and is consistent with previously obtained X-ray crystal structures of analogous  $\text{Pd}^{2+}$  coordination spheres<sup>[44, 49]</sup> (ESI†, Figures S4.1 and S4.2). This rationale is also consistent with the broadening of the  $\text{H}_a$  proton depending on halide fluctuality and temperature. Interestingly, the magnitude of the chemical shift is in inverse order from the order of the electronegativity of the halides, but we note that the growing ionic radius moving down the series gives increased spatial overlap between  $\text{H}_a$  and the acceptor (from the DFT structures, an increase of 0.12 Å of overlap going from Cl through Br to I). We hoped to use electrochemistry to further probe the effect of halide identity upon the electronics of the system, but unfortunately the broad and strong peaks associated with redox processes of the halides prevent sensible insight.

Interestingly, the formation of oligomeric structures/untidy spectra with the  $[\text{Pd}_2\text{L}_2\text{X}_2]^{2+}$  at higher concentrations was not observed: up to a 20 mM concentration the spectra remained well defined (ESI†, Figure S2.29). Potentially this is due to the preference for the halides for the site *cis* to the pyridyl ring from the bidentate site of **L** due to hydrogen bonding, whereas with  $\text{L}' = \text{DMSO}$ , larger oligomers may show a variety of binding positions.

With the ability to generate  $[\text{Pd}_2\text{L}_2\text{X}_2]^{2+}$  macrocycles *in situ* confirmed, and insight into their character obtained, we now sought to investigate whether or not their formation was reversible. Two equivalents of  $\text{AgBF}_4$  per complex were added to the solutions (Figure 2 *bottom*). In the case of bromide and iodide, this resulted in the formation of an  $\text{AgX}$  precipitate which was removed by centrifugation. The  $^1\text{H}$  NMR spectra of

the samples showed reformation of the tetracationic  $[\text{Pd}_2\text{L}_2(\text{DMSO})_2]^{4+}$  species (ESI†, Figure S2.28). For  $[\text{Pd}_2\text{L}_2\text{Cl}_2]^{2+}$  however, neither precipitation nor spectral changes were observed. Leaving the solution for a prolonged period (>10 days) or heating at  $60^\circ\text{C}$  overnight also caused no change (ESI†, Figure S2.28). Therefore, while the *in situ* formation of  $[\text{Pd}_2\text{L}_2\text{X}_2]^{2+}$  is reversible for bromide and iodide, it is non-reversible for chloride. As chloride-containing mixtures were seen to rearrange in solution, this cannot be fully explained by the lower lability of this ligand, and hence must be for thermodynamic reasons, aided by the sparingly soluble nature of  $\text{AgX}$  salts in DMSO.<sup>[50]</sup> An analysis of the energies of products minus reactants for the formation of the dihalide species supported the idea that the chloride complex was the most thermodynamically favoured (ESI†, S3).

### Supramolecular Interactions

We planned to investigate the influence of charge difference between the complexes upon molecular recognition. We were also very interested to see whether the differing strength of hydrogen bond to the ancillary ligand could be exploited to alter binding affinities: we do not believe that this has been previously demonstrated or explored. For solubility reasons, we carried out these investigations in DMSO.

To explore this idea, we designed a 'guest' for our studies (note that in this study the terms 'host' and 'guest' are somewhat arbitrary, we use them for convenience to refer to the dipalladium complexes and the diplatinate complex (see below) respectively). The affinity for planar, electron-deficient cationic panels for electron rich aromatic guests is well established.<sup>[14b, 43, 51]</sup> We envisaged that both the overall cationic charge of the complex and the strength of the hydrogen bond for the halide complexes would influence this affinity.

We therefore synthesised  $[(\text{bis}-(\text{E}-2-((2\text{-oxidobenzylidene})\text{-amino})\text{-phenolate})\text{platinum(II)})1,6\text{-diamino-hexane}]$  (**2Pt**, Figure 7 *top*), synthesised by analogous methods to similar reported compounds<sup>[29a, 52]</sup> (ESI† S2.6, yield 89%) to explore the general validity of our idea. **2Pt** consists of two  $[(\text{E}-2-((2\text{-oxidobenzylidene})\text{-amino})\text{-phenolate})\text{platinum(II)}]$  panels joined by a 1,6-diaminohexane linker, giving suitable spatial separation between the panels to allow each to simultaneously interact with the two planar cationic panels at each end of the host(s).

Solutions of the  $[\text{Pd}_2\text{L}_2\text{L}'_2]^{n+}$  hosts (at 2.5 mM) in  $[\text{D}_6]\text{DMSO}$  were treated with two equivalents of **2Pt**.<sup>[53]</sup> The resultant solutions displayed changes in chemical shifts in the  $^1\text{H}$  NMR spectra for both hosts and guest (Figure 7 *below a – e*, ESI† S5.2).<sup>[54]</sup> The significant alterations in chemical shift for **2Pt** were those proximal to the imine (resonances 4, 5 and 6) and those from the diaminoethyl chain (resonances  $\text{NH}_2$ , 10, 11, and 12). These shifted upfield in comparison to the 'free' guest. For the hosts, the most significant shifts were also upfield, and were those from resonances a, d, and e, all located on the planar cationic panel. Interestingly, some resonances from the phenyl pyridyl arm (j, k, and in some cases l) moved upfield. The magnitude of

shifts for both host and guest was greatest for  $L' = \text{DMSO}$  (for example  $\Delta\delta(\text{H}_a) = -0.73$  ppm,  $\Delta\delta(\text{H}_d) = -0.49$  ppm,  $\Delta\delta(\text{H}_5) = -0.16$  ppm) and was ordered  $\text{DMSO} > \text{I}^- > \text{Br}^- > \text{Cl}^-$ .

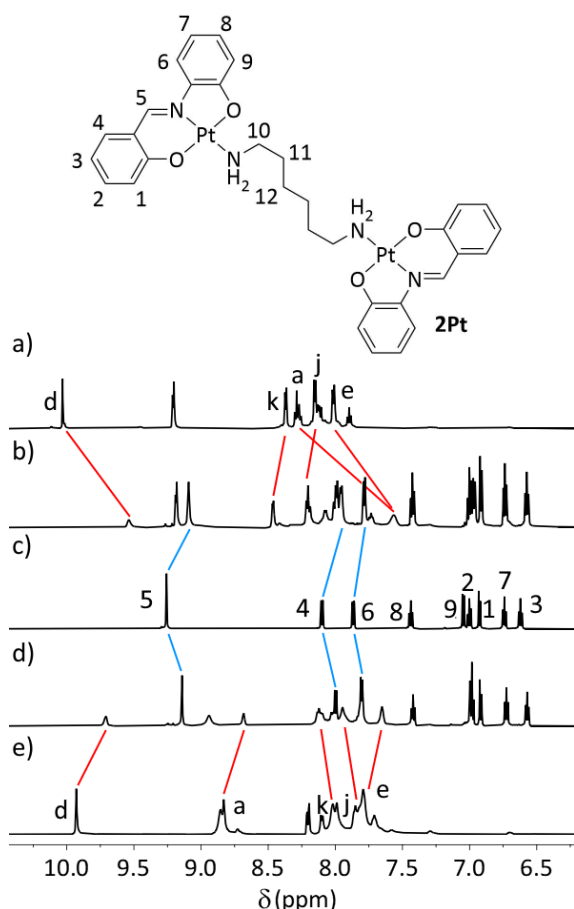


**Figure 7** top: chemical structure of guest **2Pt**, bottom: Partial stacked  $^1\text{H}$  NMR spectra (600 MHz,  $[\text{D}_2]\text{DMSO}$ , 298 K) of a)  $[\text{Pd}_2\text{L}_2(\text{DMSO})_2]^{4+}$ , b)  $[\text{Pd}_2\text{L}_2(\text{DMSO})_2]^{4+} + 2$  eq. **2Pt**, c) **2Pt**, d)  $[\text{Pd}_2\text{L}_2\text{Br}_2]^{2+} + 2$  eq. **2Pt**, and e)  $[\text{Pd}_2\text{L}_2\text{Br}_2]^{2+}$ . Only key peaks are labelled: full assignments are given in the ESI $^\dagger$ .

Assessment of binding stoichiometry and affinity between the complexes and **2Pt** was unfortunately not possible using the global set of host resonances. This was because in many cases, crowding or overlapping of peaks prevented accurate determination of chemical shift. Only the chemical shifts of the  $\text{H}_d$  and  $\text{H}_i$  proton resonances for the hosts were able to be obtained accurately across all cases in the titrations. Therefore, these two resonances were used to assess binding models. Comparison of residuals for the two 1:2 models with sensible results/reasonable errors (non-cooperative and statistical) and the 1:1 model gave lowest errors for the 1:2 non-cooperative model (ESI $^\dagger$ , S5.1).<sup>[55]</sup> Analysis *via* HR ESI-MS (DMSO/acetonitrile) from direct injection of the samples showed association between the  $[\text{Pd}_2\text{L}_2\text{L}'_2]^{n+}$  complexes and **2Pt**, with both the 1:1  $[(\text{2Pt})\text{C}(\text{host})]^{n+}$  adduct (for example, for  $L' = \text{I}^-$ ,  $n = 2$ ,  $m/z = 1235.1770$ ) and the 1:2  $[(\text{2Pt})_2\text{C}(\text{host})]^{n+}$  adduct ( $L' = \text{I}^-$ ,  $n = 2$ ,  $m/z = 1699.2838$ ) being present (ESI $^\dagger$  Figure S5.19). Recently, problems with the use of the Job plot for stoichiometric determination have been identified. These relate primarily to inaccuracies in determining stoichiometry for 1:2 or higher stoichiometries.<sup>[56]</sup> But the same publications outlining

these problems also note that a 1:1 binding stoichiometry generally gives a correct answer. Divergence from a 1:1 stoichiometry is therefore evidence that 1:1 binding may not be correct. We carried out the mole ratio titration<sup>[57]</sup> variant, using  $^1\text{H}$  NMR spectroscopy at  $[\text{host}] = 2.5$  mM. The triazole proton resonance  $\text{H}_d$  was, across all hosts, the peak least obstructed by other environments during the titrations, and so was used to assess binding stoichiometry, which for all host complexes was a 1:2 host/guest ratio (Figure 8, ESI $^\dagger$  Figure S5.20). While this is not conclusive evidence of 1:2 binding, it suggests that a 1:1 stoichiometry is not correct. On the basis of the residual analysis for the two proton resonances of which we could obtain accurate data, the mass spectrometry, and with the subsidiary technique of the mole ratio method, we assign the binding stoichiometry as 1:2. We also think that an alternative 2:1 binding stoichiometry between host and guest is unlikely: it would involve two cationic complexes sandwiching the diplatinate guest, which would result in some degree of electrostatic repulsion, and also there is no evidence of this via mass spectrometry. From the  $^1\text{H}$  NMR titration data, these 1:2 binding constants were best described as non-cooperative (ESI $^\dagger$ , S5.5).<sup>[55-56]</sup> The value (and order) of  $K_{11}$  across the series was:  $L' = \text{DMSO}$  ( $K = 680 \pm 60 \text{ M}^{-1}$ ), iodide ( $K = 440 \pm 30 \text{ M}^{-1}$ ), bromide ( $K = 250 \pm 20 \text{ M}^{-1}$ ), then chloride ( $K = 179 \pm 5 \text{ M}^{-1}$ ). Being a non-cooperative system,  $K_{12}$  is one quarter of  $K_{11}$ . These are not high affinities even for a neutral guest,<sup>[58]</sup> but the key fact here is that it is clear from these data that the identity of  $L'$  influences the interaction between the host and **2Pt**, and gives statistically significant differences in binding affinity. As previously stated, the affinity between electron-rich and electron-poor aromatics through  $\pi$ - $\pi$  interactions is well established.

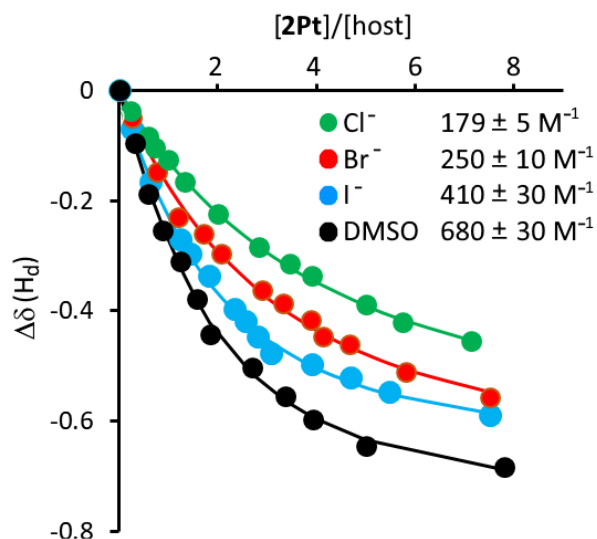


**Figure 8** Plot showing the changes in chemical shift (600 MHz,  $[\text{D}_2]\text{DMSO}$ , 298 K,  $[\text{host}] = 2.5$  mM) of resonance  $\text{H}_d$  of  $[\text{Pd}_2\text{L}_2\text{L}'_2]^{n+}$  species ( $L' = \text{DMSO}$ , iodide, bromide or chloride) upon sequential addition of **2Pt**. Curves are fitted from a 1:2 non-cooperative model. The stated constants are for  $K_{11}$ ,  $K_{12}$  is in all cases one quarter of these values. The observed and calculated shifts are shown for  $\text{H}_d$ ,  $\text{H}_i$  was also included in the analysis.

The stronger affinity for the tetracationic complex with ligated DMSO solvent versus dicationic complexes with bound halides

is consistent with this. The ordering of the binding constants for the halides ( $I^- > Br^- > Cl^-$ ) also follows this trend. As the chemical shift of the  $H_a$  proton moves further downfield with increasing ionic radius of the halide, so too does the electron deficiency of the planar cationic panel. This is reflected in the higher affinity between host and guest.

Regrettably, despite numerous efforts crystals of the host/guest adducts were not obtained. Fortunately, through-space NMR techniques were successfully employed to establish the host/guest binding mode. Through-space coupling in systems employing  $\pi$ - $\pi$  interactions with non-cavity binding are sometimes difficult to obtain, due to the lack of positional specificity of  $\pi$ -stacked components that are free to slide across one another, and the spatial separation between proton resonances ( $\sim 3.5$  Å) involved in these interactions. Pleasingly, this was not the case here.  $^1H$  NMR NOESY spectroscopy of  $[(2Pt)_2 \subset Pd_2L_2(DMSO)_2]^{4+}$  revealed coupling between the diaminohexane linker of **2Pt** and the (phenyl)pyridine arm of the host (Figure 8 top). This indicates that the guest lies across the surface of the host as designed, with the alkyl region atop the (phenyl)pyridyl arms, and the two panels of the guest lying against the two panels of the host.

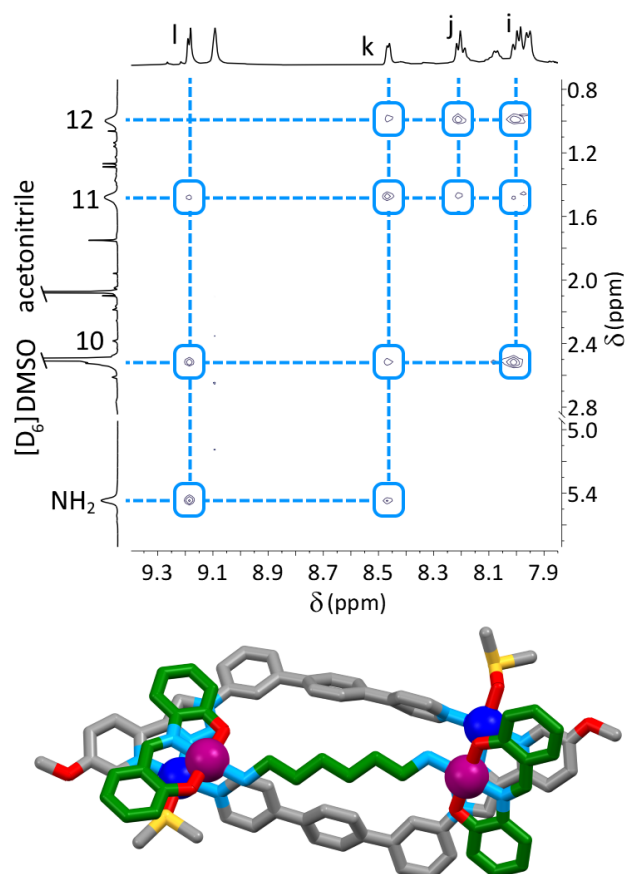


**Figure 9** top Partial  $^1H$  NOESY 2D spectrum (600 MHz,  $[D_6]DMSO$ , 298 K, 300 ms mixing time) of  $[(2Pt)_2 \subset Pd_2L_2(solvent)_2]^{4+}$ , bottom DFT model of  $[2Pt \subset Pd_2L_2(DMSO)_2]^{4+}$  from above. Colours: Carbon grey for host, green for guest, nitrogen light blue, oxygen red, palladium dark blue, platinum purple, sulphur yellow. Hydrogen atoms and solubilising chains omitted for clarity. The solubilising chain was curtailed to a methoxy group for computational simplicity.

DFT calculations of the 1:1 adduct ((BP86/def2-SVP, Figure 9 bottom) showed that this interaction mode was plausible, as did MMFF<sup>[59]</sup> models of the 1:2 adduct (ESI<sup>†</sup>). This orientation is also consistent with the downfield shifts of the proton resonances j and k, which are positioned to hydrogen bond to the oxygen atoms of **2Pt**. To establish if the same binding mode was present for the halide complexes, similar NOE couplings were observed for  $[(2Pt)_2 \subset Pd_2L_2Br_2]^{2+}$ , although the correlations were weaker (ESI<sup>†</sup> Figure S5.8).

Lastly, we used the appropriate halide sources and  $AgBF_4$  to cycle between the different host/guest adducts: through  $L' = DMSO, I^-, DMSO, Br^-$  and  $Cl^-$  (ESI<sup>†</sup> Figure 5.11). Starting with  $[(2Pt)_2 \subset Pd_2L_2(DMSO)_2]^{4+}$ , two equivalents of iodide were added. The spectrum obtained was effectively the same as for that obtained for  $[(2Pt)_2 \subset Pd_2L_2I_2]^{2+}$ .  $AgBF_4$  (2 equivalents) was then added, precipitating  $AgI$ , which was removed *via* centrifugation, returning to  $[(2Pt)_2 \subset Pd_2L_2(DMSO)_2]^{4+}$ . This process was then repeated for bromide and chloride. We were therefore able to access *in situ* four different settings of binding affinity between the guest and the core host structure, although again the  $[Pd_2L_2Cl_2]^{2+}$  complex could not be returned to  $[Pd_2L_2(DMSO)_2]^{4+}$ .

## Conclusions

In this study we use  $Pd^{2+}$  with a ligand that has both a bidentate and monodentate site to form a [2 + 2] metallo-macrocyclic. Each  $Pd^{2+}$  ion lies in a planar cationic panel, with one site from its coordination sphere occupied by an ancillary monodentate ligand. There has been a considerable drive in the field to create structurally complex and intricate assemblies, with beautiful results.<sup>[60]</sup> In contrast, this complex is unashamedly simple in structure. The complexity of this system is not derived from structure, but instead from the variability of the ancillary ligand. Through varying the identity of this ligand between solvent and the halides chloride, bromide and iodide, we were able to alter the overall charge of the complex between tetracationic (solvent) and dicationic (halides). The identity of the halide was also crucial to the character of the complex. Large differences in the  $^1H$  NMR chemical shift of the  $H_a$  proton suggest that with movement down the periodic table, significant differences in the strength of hydrogen bonding to the halide occur. These differences result in differing levels of electron deficiency of the cationic panel.

In proof-of-concept that these differences translate into varied recognition characteristics, the complexes all bound a neutral diplatinate(II) guest which consisted of two electron-rich panels joined by a diaminoalkyl linker of appropriate size to allow interaction between both sets of panels from host and guest. The affinity between host and guest was dependent on the identity of the ancillary ligand. The tetracationic complex displayed highest affinity, with the dicationic complexes arrayed  $I^- > Br^- > Cl^-$ . The system therefore has four settings of binding affinity, although the fourth (chloride) cannot be reversed from. The differences in affinity in this first generation



are admittedly small: we expect these to improve with subsequent iterations, through altering the electronic character of the host(s) and the solvent system the studies are carried out in. In comparison to the examples from the literature discussed in the introduction (both those retaining and altering core structure), host-guest binding cannot be completely 'turned off' in this iteration, but instead takes place on a 'sliding scale'.

We have therefore shown that even simple systems can be employed to generate stimuli-responsive, nuanced, and controlled multi-step complexity over a molecular recognition event. Events of this nature lie at the core of signalling, sensing, catalytic and photophysical functions both in nature and the laboratory. While the binding of this particular guest fulfils no function, it demonstrates the capacity for utilisation of this system for numerous applications. For example, both the Peris group<sup>[14c]</sup> and ourselves<sup>[14b]</sup> have recently bound substrates within metallosupramolecular systems using  $\pi$ - $\pi$  interactions and then carried out chemical transformations upon them. Graduated control over these processes can only result in the development of more powerfully and precisely tuned systems, and we expect this work to provide new tools to allow a finer touch in their development.

Lastly, this work utilises a novel method for influencing molecular recognition. Hydrogen bonding has previously been used to (non-reversibly) alter host character, in allosteric<sup>[61]</sup> binding of *exo* guests to lower affinity for hydrogen-bonded encapsulated *endo* guests in cages.<sup>[62]</sup> Our study differs from this not only in that the hydrogen bonding acceptor is now ligated to the complex, but also in that this process is (in most cases) reversible. Furthermore, here the role of the hydrogen bonding event is to strengthen affinity for aromatic guests through  $\pi$ - $\pi$  interactions. A key design feature in this regard is the planarity of the surface consisting of metal ion, bidentate site, and ancillary ligand. As pointed out above,  $\pi$ - $\pi$  interactions can and have been employed to achieve multiple goals. The general system used here can easily be extended to a range of polynuclear metallosupramolecular systems. It can also be applied to mononuclear analogues. We are currently working on a number of these avenues.

## Conflicts of interest

There are no conflicts to declare.

## Acknowledgements

DP would like to thank the ARC for a DECRA Fellowship, and the Royal Society of New Zealand for a Rutherford Postdoctoral Fellowship. BH would like to gratefully acknowledge the MBIE Catalyst Fund for a PhD scholarship. RV would like to thank the University of Otago for a PhD scholarship. The authors would like to thank the Australia National University, the University of Canterbury, the University of Otago, and the MacDiarmid Institute for additional funding. The authors acknowledge the

contribution of the NeSI high performance computing facilities to the results of this research. New Zealand's national facilities are provided by the New Zealand eScience Infrastructure and funded jointly by NeSI's collaborator institutions and through the Ministry of Business, Innovation & Employment's Research Infrastructure program. URL: <https://www.nesi.org.nz>.

## References

- [1] a) L. C. Myers, R. D. Kornberg, "Mediator of transcriptional regulation", *Annu. Rev. Biochem.* **2000**, *69*, 729-749; b) C. Weigel, A. Schmidt, B. Ruckert, R. Lurz, W. Messer, "DnaA protein binding to individual DnaA boxes in the Escherichia coli replication origin, oriC", *EMBO J.* **1997**, *16*, 6574-6583; c) F. Werner, D. Grohmann, "Evolution of multisubunit RNA polymerases in the three domains of life", *Nat. Rev. Microbiol.* **2011**, *9*, 85-98.
- [2] E. C. Theil, "Ferritin: structure, gene regulation, and cellular function in animals, plants, and microorganisms", *Annu. Rev. Biochem.* **1987**, *56*, 289-315.
- [3] a) A. N. Schechter, "Hemoglobin research and the origins of molecular medicine", *Blood* **2008**, *112*, 3927-3938; b) R. D. Vale, "The Molecular Motor Toolbox for Intracellular Transport", *Cell* **2003**, *112*, 467-480.
- [4] L. Hedstrom, "Serine protease mechanism and specificity", *Chem. Rev.* **2002**, *102*, 4501-4524.
- [5] G. M. Cooper, *The Cell: A Molecular Approach*, 2nd edition ed., Sinauer Associates, Sunderland (MA), **2000**.
- [6] a) H. Nishi, A. Shaytan, A. R. Panchenko, "Physicochemical mechanisms of protein regulation by phosphorylation", *Front. Genet.* **2014**, *5*; b) P. Hauske, C. Ottmann, M. Meltzer, M. Ehrmann, M. Kaiser, "Allosteric Regulation of Proteases", *ChemBioChem* **2008**, *9*, 2920-2928.
- [7] M. J. Lee, M. B. Yaffe, "Protein Regulation in Signal Transduction", *CSH Perspect. Biol.* **2016**, *8*, a005918.
- [8] a) S. Zarra, D. M. Wood, D. A. Roberts, J. R. Nitschke, "Molecular containers in complex chemical systems", *Chem. Soc. Rev.* **2015**, *44*, 419-432; b) R. A. S. Vasdev, D. Preston, J. D. Crowley, "Multicavity Metallosupramolecular Architectures", *Chem. Asian J.* **2017**, *12*, 2513-2523.
- [9] a) P. Mal, B. Breiner, K. Rissanen, J. R. Nitschke, "White phosphorus is air-stable within a self-assembled tetrahedral capsule", *Science* **2009**, *324*, 1697-1699; b) M. Yamashina, Y. Sei, M. Akita, M. Yoshizawa, "Safe storage of radical initiators within a polyaromatic nanocapsule", *Nat. Commun.* **2014**, *5*, 4662.
- [10] I. A. Riddell, M. M. Smulders, J. K. Clegg, J. R. Nitschke, "Encapsulation, storage and controlled release of sulfur hexafluoride from a metal-organic capsule", *Chem. Commun.* **2011**, *47*, 457-459.
- [11] C. G. Taylor, J. R. Piper, M. D. Ward, "Binding of chemical warfare agent simulants as guests in a coordination cage: contributions to binding and a fluorescence-based response", *Chem. Commun.* **2016**, *52*, 6225-6228.
- [12] a) B. Therrien, G. Suss-Fink, P. Govindaswamy, A. K. Renfrew, P. J. Dyson, "The "complex-in-a-complex" cations [(acac)<sub>2</sub>CrRu<sub>6</sub>(p-*i*PrC<sub>6</sub>H<sub>4</sub>Me)<sub>6</sub>(tpt)<sub>2</sub>(d**h**bq)<sub>3</sub>]<sup>6+</sup>: A trojan horse for cancer cells", *Angew. Chem. Int. Ed. Engl.* **2008**, *47*, 3773-3776; b) Y. R. Zheng, K. Suntharalingam, T. C. Johnstone, S. J. Lippard, "Encapsulation of Pt(IV) Prodrugs within a Pt(II) Cage for Drug Delivery", *Chem. Sci.* **2015**, *6*,

- 1189-1193; c) J. E. M. Lewis, E. L. Gavey, S. A. Cameron, J. D. Crowley, "Stimuli-responsive Pd<sub>2</sub>L<sub>4</sub> metallosupramolecular cages: towards targeted cisplatin drug delivery", *Chem. Sci.* **2012**, *3*, 778-784.
- [13] B. P. Burke, W. Grantham, M. J. Burke, G. S. Nichol, D. Roberts, I. Renard, R. Hargreaves, C. Cawthorne, S. J. Archibald, P. J. Lusby, "Visualizing Kinetically Robust CoIII4L6 Assemblies in Vivo: SPECT Imaging of the Encapsulated [<sup>99m</sup>Tc]TcO<sub>4</sub><sup>-</sup> Anion", *J. Am. Chem. Soc.* **2018**, *140*, 16877-16881.
- [14] a) V. Marti-Centelles, A. L. Lawrence, P. J. Lusby, "High Activity and Efficient Turnover by a Simple, Self-Assembled "Artificial Diels-Alderase"", *J. Am. Chem. Soc.* **2018**, *140*, 2862-2868; b) D. Preston, J. J. Sutton, K. C. Gordon, J. D. Crowley, "A Nona-nuclear Heterometallic Pd<sub>3</sub>Pt<sub>6</sub> "Donut"-Shaped Cage: Molecular Recognition and Photocatalysis", *Angew. Chem. Int. Ed. Engl.* **2018**, *57*, 8659-8663; c) V. Martínez-Agramunt, E. Peris, "Photocatalytic Properties of a Palladium Metallosquare with Encapsulated Fullerenes via Singlet Oxygen Generation", *Inorg. Chem.* **2019**; d) C. Colombar, C. Fuertes-Espinosa, S. Goeb, M. Salle, M. Costas, L. Blancafort, X. Ribas, "Self-Assembled Cofacial Zinc-Porphyrin Supramolecular Nanocapsules as Tuneable <sup>1</sup>O<sub>2</sub> Photosensitizers", *Chem. Eur. J.* **2018**, *24*, 4371-4381; e) W. Cullen, M. C. Misuraca, C. A. Hunter, N. H. Williams, M. D. Ward, "Highly efficient catalysis of the Kemp elimination in the cavity of a cubic coordination cage", *Nat. Chem.* **2016**, *8*, 231; f) J. Guo, Y. Z. Fan, Y. L. Lu, S. P. Zheng, C. Y. Su, "Visible-Light Photocatalysis of Asymmetric [2+2] Cycloaddition in Cage-Confined Nanospace Merging Chirality with Triplet-State Photosensitization", *Angew. Chem. Int. Ed. Engl.* **2020**, *59*, 8661-8669.
- [15] a) Y. Nishioka, T. Yamaguchi, M. Yoshizawa, M. Fujita, "Unusual [2+4] and [2+2] cycloadditions of arenes in the confined cavity of self-assembled cages", *J. Am. Chem. Soc.* **2007**, *129*, 7000-7001; b) T. Kusakawa, T. Nakai, T. Okano, M. Fujita, "Remarkable acceleration of Diels-Alder reactions in a self-assembled coordination cage", *Chem. Lett.* **2003**, *32*, 284-285; c) M. Yoshizawa, Y. Takeyama, T. Okano, M. Fujita, "Cavity-directed synthesis within a self-assembled coordination cage: highly selective [2 + 2] cross-photodimerization of olefins", *J. Am. Chem. Soc.* **2003**, *125*, 3243-3247.
- [16] a) W. Wang, Y. X. Wang, H. B. Yang, "Supramolecular transformations within discrete coordination-driven supramolecular architectures", *Chem. Soc. Rev.* **2016**, *45*, 2656-2693; b) T. Y. Kim, R. A. S. Vasdev, D. Preston, J. D. Crowley, "Strategies for Reversible Guest Uptake and Release from Metallosupramolecular Architectures", *Chem. Eur. J.* **2018**, *24*, 14878-14890.
- [17] Stimuli have also been directed towards the guest molecule, thereby altering host-guest affinity, see; a) W. Cullen, S. Turega, C. A. Hunter, M. D. Ward, "pH-dependent binding of guests in the cavity of a polyhedral coordination cage: reversible uptake and release of drug molecules", *Chem. Sci.* **2015**, *6*, 625-631; b) W. Cullen, K. A. Thomas, C. A. Hunter, M. D. Ward, "pH-Controlled selection between one of three guests from a mixture using a coordination cage host", *Chem. Sci.* **2015**, *6*, 4025-4028; c) C. Colombar, G. Szaloki, M. Allain, L. Gomez, S. Goeb, M. Salle, M. Costas, X. Ribas, "Reversible C<sub>60</sub> Ejection from a Metallocage through the Redox-Dependent Binding of a Competitive Guest", *Chem. Eur. J.* **2017**, *23*, 3016-3022; d) W. Y. Sun, T. Kusakawa, M. Fujita, "Electrochemically driven clathration/declathration of ferrocene and its derivatives by a nanometer-sized coordination cage", *J. Am. Chem. Soc.* **2002**, *124*, 11570-11571; e) G. H. Clever, M. Shionoya, "A pH switchable pseudorotaxane based on a metal cage and a bis-anionic thread", *Chem. Eur. J.* **2010**, *16*, 11792-11796; f) G. H. Clever, S. Tashiro, M. Shionoya, "Light-triggered crystallization of a molecular host-guest complex", *J. Am. Chem. Soc.* **2010**, *132*, 9973-9975.
- [18] S. M. Jansze, G. Cecot, K. Severin, "Reversible disassembly of metallasupramolecular structures mediated by a metastable-state photoacid", *Chem. Sci.* **2018**, *9*, 4253-4257.
- [19] V. Croue, S. Goeb, G. Szaloki, M. Allain, M. Salle, "Reversible Guest Uptake/Release by Redox-Controlled Assembly/Disassembly of a Coordination Cage", *Angew. Chem. Int. Ed. Engl.* **2016**, *55*, 1746-1750.
- [20] Q. Gan, T. K. Ronson, D. A. Vosburg, J. D. Thoburn, J. R. Nitschke, "Cooperative loading and release behavior of a metal-organic receptor", *J. Am. Chem. Soc.* **2015**, *137*, 1770-1773.
- [21] N. Kishi, M. Akita, M. Yoshizawa, "Selective host-guest interactions of a transformable coordination capsule/tube with fullerenes", *Angew. Chem. Int. Ed. Engl.* **2014**, *53*, 3604-3607.
- [22] a) D. Preston, A. Fox-Charles, W. K. Lo, J. D. Crowley, "Chloride triggered reversible switching from a metallosupramolecular [Pd<sub>2</sub>L<sub>4</sub>]<sup>4+</sup> cage to a [Pd<sub>2</sub>L<sub>2</sub>Cl<sub>4</sub>] metallo-macrocyclic with release of endo- and exo-hedrally bound guests", *Chem. Commun.* **2015**, *51*, 9042-9045; b) C. S. Wood, C. Browne, D. M. Wood, J. R. Nitschke, "Fuel-Controlled Reassembly of Metal-Organic Architectures", *ACS Cent. Sci.* **2015**, *1*, 504-509.
- [23] a) S. Zarra, J. K. Clegg, J. R. Nitschke, "Selective assembly and disassembly of a water-soluble Fe<sub>10</sub>L<sub>15</sub> prism", *Angew. Chem. Int. Ed. Engl.* **2013**, *52*, 4837-4840; b) N. Kishi, M. Akita, M. Kamiya, S. Hayashi, H. F. Hsu, M. Yoshizawa, "Facile catch and release of fullerenes using a photoresponsive molecular tube", *J. Am. Chem. Soc.* **2013**, *135*, 12976-12979.
- [24] T. Murase, S. Sato, M. Fujita, "Switching the interior hydrophobicity of a self-assembled spherical complex through the photoisomerization of confined azobenzene chromophores", *Angew. Chem. Int. Ed. Engl.* **2007**, *46*, 5133-5136.
- [25] A. K. Chan, W. H. Lam, Y. Tanaka, K. M. Wong, V. W. Yam, "Multiaddressable molecular rectangles with reversible host-guest interactions: modulation of pH-controlled guest release and capture", *Proc. Natl. Acad. Sci. USA* **2015**, *112*, 690-695.
- [26] Y. Sakata, M. Okada, M. Tamiya, S. Akine, "Post-Metalation Modification of a Macrocyclic Dicobalt(III) Metallohost by Site-Selective Ligand Exchange for Guest Recognition Control", *Chem. Eur. J.*, **2020**, *26*, 7595-7601.
- [27] a) T. R. Cook, P. J. Stang, "Recent Developments in the Preparation and Chemistry of Metallacycles and Metallacages via Coordination", *Chem. Rev.* **2015**, *115*, 7001-7045; b) K. Harris, D. Fujita, M. Fujita, "Giant hollow M<sub>n</sub>L<sub>n</sub> spherical complexes: structure, functionalisation and applications", *Chem. Commun.* **2013**, *49*, 6703-6712; c) N. B. Debata, D. Tripathy, D. K. Chand, "Self-assembled

- coordination complexes from various palladium(II) components and bidentate or polydentate ligands", *Coord. Chem. Rev.* **2012**, *256*, 1831-1945; d) D. Preston, P. E. Kruger, "Using Complementary Ligand Denticity to Direct Metallosupramolecular Structure about Metal Ions with Square-Planar Geometry", *Chempluschem* **2020**, *85*, 454-465; e) J. E. M. Lewis, J. D. Crowley, "Metallo-Supramolecular Self-Assembly with Reduced-Symmetry Ligands", *Chempluschem* **2020**, *85*, 815-827.
- [28] a) A. Torres-Huerta, J. Cruz-Huerta, H. Höpfl, L. G. Hernández-Vázquez, J. Escalante-García, A. Jiménez-Sánchez, R. Santillan, I. F. Hernández-Ahuactzi, M. Sánchez, "Variation of the Molecular Conformation, Shape, and Cavity Size in Dinuclear Metalla-Macrocycles Containing Hetero-Ditopic Dithiocarbamate-Carboxylate Ligands from a Homologous Series of N-Substituted Amino Acids", *Inorg. Chem.* **2016**, *55*, 12451-12469; b) W. W. H. Wong, D. Curiel, A. R. Cowley, P. D. Beer, "Dinuclear zinc(II) dithiocarbamate macrocycles: ditopic receptors for a variety of guest molecules", *Dalton Trans.* **2005**, 359-364; c) D. Preston, R. A. Tucker, A. L. Garden, J. D. Crowley, "Heterometallic  $[M_nPt_n(L)_{2n}]^{x+}$  Macrocycles from Dichloromethane-Derived Bis-2-pyridyl-1,2,3-triazole Ligands", *Inorg. Chem.* **2016**, *55*, 8928-8934; d) J. A. Findlay, C. J. McAdam, J. J. Sutton, D. Preston, K. C. Gordon, J. D. Crowley, "Metallosupramolecular Architectures Formed with Ferrocene-Linked Bis-Bidentate Ligands: Synthesis, Structures, and Electrochemical Studies", *Inorg. Chem.* **2018**, *57*, 3602-3614; e) C. E. Miron, M. R. Colden Leung, E. I. Kennedy, O. Fleischel, M. A. Khorasani, N. Wu, J. L. Mergny, A. Petitjean, "Closing the Loop: Triazolopyridine Coordination Drives the Self-Assembly of Metallomacrocycles with Tunable Topologies for Small-Molecule and Guanine-Quadruplex Recognition", *Chem. Eur. J.* **2018**, *24*, 18718-18734; f) N. Komiya, T. Muraoka, M. Iida, M. Miyanaga, K. Takahashi, T. Naota, "Ultrasound-Induced Emission Enhancement Based on Structure-Dependent Homo- and Heterochiral Aggregations of Chiral Binuclear Platinum Complexes", *J. Am. Chem. Soc.* **2011**, *133*, 16054-16061.
- [29] a) J. D. Crowley, A. J. Goshe, B. Bosnich, "Molecular recognition. Electrostatic effects in supramolecular self-assembly", *Chem. Commun.* **2003**, 392-393; b) C. García-Simón, M. García-Borràs, L. Gómez, T. Parella, S. Osuna, J. Juanhuix, I. Imaz, D. MasPOCH, M. Costas, X. Ribas, "Sponge-like molecular cage for purification of fullerenes", *Nat. Commun.* **2014**, *5*, 5557; c) R. Lavendomme, T. K. Ronson, J. R. Nitschke, "Metal and Organic Templates Together Control the Size of Covalent Macrocycles and Cages", *J. Am. Chem. Soc.* **2019**, *141*, 12147-12158; d) R. Trokowski, S. Akine, T. Nabeshima, "Synthesis, characterization and molecular recognition of a bis-platinum terpyridine dimer", *Chem. Commun.* **2008**, 889-890; e) D. Preston, A. R. Inglis, A. L. Garden, P. E. Kruger, "A symmetry interaction approach to  $[M_2L_2]^{4+}$  metallocycles and their self-catenation", *Chem. Commun.* **2019**, *55*, 13271-13274.
- [30] a) M. Fujita, O. Sasaki, T. Mitsuhashi, T. Fujita, J. Yazaki, K. Yamaguchi, K. Ogura, "On the structure of transition-metal-linked molecular squares", *Chem. Commun.* **1996**, 1535-1536; b) O. Domarco, C. Kieler, C. Pirker, C. Dinhof, B. Englinger, J. M. Reisecker, G. Timelthaler, M. D. García, C. Peinador, B. K. Keppler, W. Berger, A. Terenzi, "Subcellular Duplex DNA and G-Quadruplex Interaction Profiling of a Hexagonal Pt<sup>II</sup> Metallocycle", *Angew. Chem.* **2019**, *131*, 8091-8096; c) S. Prusty, S. Krishnaswamy, S. Bandi, B. Chandrika, J. Luo, J. S. McIndoe, G. S. Hanan, D. K. Chand, "Reversible Mechanical Interlocking of D-Shaped Molecular Karabiners bearing Coordination-Bond Loaded Gates: Route to Self-Assembled [2]Catenanes", *Chem. Eur. J.* **2015**, *21*, 15174-15187; d) V. Martínez-Agramunt, T. Eder, H. Darmandeh, G. Guisado-Barrios, E. Peris, "A Size-Flexible Organometallic Box for the Encapsulation of Fullerenes", *Angew. Chem. Int. Ed.* **2019**, *58*, 5682-5686; e) V. Blanco, M. D. Garcia, A. Terenzi, E. Pia, A. Fernandez-Mato, C. Peinador, J. M. Quintela, "Complexation and extraction of PAHs to the aqueous phase with a dinuclear Pt(II) diazapyrenium-based metallocycle", *Chem. Eur. J.* **2010**, *16*, 12373-12380; f) C. Alvaríño, C. Platas-Iglesias, V. Blanco, M. D. García, C. Peinador, J. M. Quintela, "Stimuli-responsive metal-directed self-assembly of a ring-in-ring complex", *Dalton Trans.* **2016**, *45*, 11611-11615; g) E. M. López-Vidal, A. Prokofjevs, I. C. Gibbs-Hall, E. J. Dale, J. M. Quintela, C. Peinador, "Studies towards the synthesis of Pd(II)-containing [2] and [3]catenanes in aqueous media", *Dalton Trans.* **2018**, *47*, 2492-2496; h) M. D. García, C. Alvaríño, E. M. López-Vidal, T. Rama, C. Peinador, J. M. Quintela, "Complexation of aromatic compounds with self-assembled Pd<sup>II</sup> and Pt<sup>II</sup> metallocycles", *Inorg. Chim. Acta* **2014**, *417*, 27-37; i) S. Ibanez, E. Peris, "Dimensional Matching versus Induced-Fit Distortions: Binding Affinities of Planar and Curved Polyaromatic Hydrocarbons with a Tetragold Metallocycle", *Angew. Chem. Int. Ed.* **2020**, *59*, 6860-6865.
- [31] S. Ganta, D. K. Chand, "Molecular Recombination Phenomena in Palladium(II)-Based Self-Assembled Complexes", *Inorg. Chem.* **2018**, *57*, 5145-5158.
- [32] a) D. A. McMorran, P. J. Steel, "The First Coordinatively Saturated, Quadruply Stranded Helicate and Its Encapsulation of a Hexafluorophosphate Anion", *Angew. Chem. Int. Ed. Engl.* **1998**, *37*, 3295-3297; b) D. Fujita, Y. Ueda, S. Sato, H. Yokoyama, N. Mizuno, T. Kumasaka, M. Fujita, "Self-Assembly of  $M_{30}L_{60}$  Icosidodecahedron", *Chem* **2016**, *1*, 91-101.
- [33] Y. Zhang, M. R. Crawley, C. E. Hauke, A. E. Friedman, T. R. Cook, "Phosphorescent Decanuclear Bimetallic Pt<sub>6</sub>M<sub>4</sub> (M = Zn, Fe) Tetrahedral Cages", *Inorg. Chem.* **2017**, *56*, 4258-4262.
- [34] X. Sun, D. W. Johnson, D. L. Caulder, R. E. Powers, K. N. Raymond, E. H. Wong, "Exploiting incommensurate symmetry numbers: rational design and assembly of  $M_2M_3L_6$  supramol. clusters with a  $C_{3h}$  symmetry", *Angew. Chem. Int. Ed.* **1999**, *38*, 1303-1307.
- [35] a) S. Hiraoka, Y. Sakata, M. Shionoya, "Ti(IV)-Centered Dynamic Interconversion between Pd(II), Ti(IV)-Containing Ring and Cage Molecules", *J. Am. Chem. Soc.* **2008**, *130*, 10058-10059; b) Y. Sakata, S. Hiraoka, M. Shionoya, "Site-Selective Ligand Exchange on a Heteroleptic Ti(IV) Complex Towards Stepwise Multicomponent Self-Assembly", *Chem. Eur. J.* **2010**, *16*, 3318-3325, S3318/S3311-S3318/S3318.
- [36] N. L. S. Yue, D. J. Eisler, M. C. Jennings, R. J. Puddephatt, "Macrocyclic and lantern complexes of palladium(II) with bis(amidopyridine) ligands: synthesis, structure, and host-guest chemistry", *Inorg. Chem.* **2004**, *43*, 7671-7681.

- [37] N. R. Lagesse, K. Y. L. Tan, J. D. Crowley, J. A. Findlay, "Planar 2-Pyridyl-1,2,3-triazole Derived Metallo-ligands: Self-assembly with PdCl<sub>2</sub> and Photocatalysis", *Chem. Asian J.* **2020**, *15*, 1567-1573.
- [38] R. Zhu, J. Lubben, B. Ditttrich, G. H. Clever, "Stepwise halide-triggered double and triple catenation of self-assembled coordination cages", *Angew. Chem. Int. Ed. Engl.* **2015**, *54*, 2796-2800.
- [39] A. K. Pal, B. Laramée-Milette, G. S. Hanan, "Self-assembly of supramolecular triangles with neutral trans-PdCl<sub>2</sub> directing units", *RSC Adv.* **2014**, *4*, 21262-21266.
- [40] Relatively recently, Clever and co-workers have reported [Pd<sub>2</sub>L<sub>3</sub>(solvent)<sub>2</sub>]<sup>4+</sup> 'bowls' where the coordination sphere of each metal ion is occupied by the monodentate sites of three linking ligands, and a solvent molecule. In this particular case, the identity of the solvent molecule does not influence ligand arrangement at the metal centre, which is instead driven by the bulk of the quinoline donors on the linking ligands. By moving to bulkier acridine donors, they were able to access [Pd<sub>2</sub>L<sub>2</sub>(solvent)<sub>2</sub>]<sup>4+</sup> macrocycles (Fig 1d) with coordinated acetonitrile molecules, and then exchange these for chloride anions to form a neutral [Pd<sub>2</sub>L<sub>2</sub>Cl<sub>2</sub>] complex. The effects of this transformation upon the recognition of guests, or its reversibility, were not explored. See; a) B. Chen, J. J. Holstein, S. Horiuchi, W. G. Hiller, G. H. Clever, "Pd(II) Coordination Sphere Engineering: Pyridine Cages, Quinoline Bowls, and Heteroleptic Pills Binding One or Two Fullerenes", *J. Am. Chem. Soc.* **2019**, *141*, 8907-8913; b) B. Chen, S. Horiuchi, J. J. Holstein, J. Tessarolo, G. H. Clever, "Tunable Fullerene Affinity of Cages, Bowls and Rings Assembled by Pd(II) Coordination Sphere Engineering", *Chem. Eur. J.* **2019**, *25*, 14921-14927.
- [41] a) B. H. Wilson, H. S. Scott, O. T. Qazvini, S. G. Telfer, C. Mathoniere, R. Clerac, P. E. Kruger, "A supramolecular porous material comprising Fe(II) mesocates", *Chem. Commun.* **2018**, *54*, 13391-13394; b) P. W. V. Butler, P. E. Kruger, J. S. Ward, "Self-assembly of M<sub>4</sub>L<sub>4</sub> tetrahedral cages incorporating pendant P=S and P=Se functionalised ligands", *Chem. Commun.* **2019**, *55*, 10304-10307; c) D. A. W. Ross, D. Preston, J. D. Crowley, "Self-Assembly with 2,6-Bis(1-(pyridin-4-ylmethyl)-1H-1,2,3-triazol-4-yl)pyridine: Silver(I) and Iron(II) Complexes", *Molecules* **2017**, *22*, 1762.
- [42] a) D. Preston, P. E. Kruger, "Reversible Transformation between a [PdL<sub>2</sub>]<sup>2+</sup> "Figure-of-Eight" Complex and a [Pd<sub>2</sub>L<sub>2</sub>]<sup>4+</sup> Dimer: Switching On and Off Self-Recognition", *Chem. Eur. J.* **2019**, *25*, 1781-1786; b) D. Preston, A. R. Inglis, J. D. Crowley, P. E. Kruger, "Self-assembly and Cycling of a Three-state Pd<sub>x</sub>L<sub>y</sub> Metallosupramolecular System", *Chem. Asian J.* **2019**, *14*, 3404-3408.
- [43] D. Preston, J. A. Findlay, J. D. Crowley, "Recognition Properties and Self-assembly of Planar [M(2-pyridyl-1,2,3-triazole)<sub>2</sub>]<sup>2+</sup> Metallo-ligands", *Chem. Asian J.* **2019**, *14*, 1136-1142.
- [44] W. K. Lo, G. S. Huff, J. R. Cubanski, A. D. Kennedy, C. J. McAdam, D. A. McMorran, K. C. Gordon, J. D. Crowley, "Comparison of inverse and regular 2-pyridyl-1,2,3-triazole "click" complexes: structures, stability, electrochemical, and photophysical properties", *Inorg. Chem.* **2015**, *54*, 1572-1587.
- [45] 86 hits in the CCDC database at 1st April 2020, including; a) M. Hosseini-Kharat, K. Karami, M. Saeidifar, C. Rizzoli, R. Zahedi-Nasab, Z. Sohrabijam, T. Sharifi, "A novel Pd(II) CNO pincer complex of MR (methyl red): synthesis, crystal structure, interaction with human serum albumin (HSA) in vitro and molecular docking", *New J. Chem.* **2017**, *41*, 9897-9907; b) Z. Wu, M. Chen, C. Chen, "Ethylene Polymerization and Copolymerization by Palladium and Nickel Catalysts Containing Naphthalene-Bridged Phosphine-Sulfonate Ligands", *Organometallics* **2016**, *35*, 1472-1479; c) D. Zhang, C. Chen, "Influence of Polyethylene Glycol Unit on Palladium- and Nickel-Catalyzed Ethylene Polymerization and Copolymerization", *Angew. Chem. Int. Ed.* **2017**, *56*, 14672-14676.
- [46] 41 hits in the CCDC database at 1st April 2020, including; a) S. E. Walker, J. Boehnke, P. E. Glen, S. Levey, L. Patrick, J. A. Jordan-Hore, A.-L. Lee, "Ligand- and Base-Free Pd(II)-Catalyzed Controlled Switching between Oxidative Heck and Conjugate Addition Reactions", *Org. Lett.* **2013**, *15*, 1886-1889; b) T. Liang, C. Chen, "Side-Arm Control in Phosphine-Sulfonate Palladium- and Nickel-Catalyzed Ethylene Polymerization and Copolymerization", *Organometallics* **2017**, *36*, 2338-2344; c) A. Bjelopetrović, S. Lukin, I. Halasz, K. Užarević, I. Đilović, D. Barišić, A. Budimir, M. Juribašić Kulcsár, M. Čurić, "Mechanism of Mechanochemical C-H Bond Activation in an Azobenzene Substrate by Pd(II) Catalysts", *Chem. Eur. J.* **2018**, *24*, 10672-10682.
- [47] We have previously reported a system with a ligand of similar dimensions but with tridentate and monodentate sites (ref 29d). At higher concentrations the dinuclear complex formed from this ligand self-catenated. There was no evidence of this behaviour here. The reasons for this difference in behaviour are not clear, but might plausibly be related to either subtle differences in cavity dimensions, or to the 'free' site at the metal ion allowing different coordination modes favouring oligomeric structures.
- [48] Adding more than two equivalents brought about spectral untidiness, indicating uncontrolled decomposition of the complexes. An excess of halide gave a spectrum matching that of the free ligand.
- [49] a) D. Schweinfurth, R. Pattacini, S. Strobel, B. Sarkar, "New 1,2,3-triazole ligands through click reactions and their palladium and platinum complexes", *Dalton Trans.* **2009**, 9291-9297; b) D. Schweinfurth, S. Strobel, B. Sarkar, "Expanding the scope of Click derived 1,2,3-triazole ligands: New palladium and platinum complexes", *Inorg. Chim. Acta* **2011**, *374*, 253-260; c) S. Jindabot, K. Teerachanan, P. Thongkam, S. Kiatisevi, T. Khamnaen, P. Phiriyawirut, S. Charoenchaidet, T. Sooksimuang, P. Kongsaree, P. Sangtrirutnugul, "Palladium(II) complexes featuring bidentate pyridine-triazole ligands: Synthesis, structures, and catalytic activities for Suzuki-Miyaura coupling reactions", *J. Organomet. Chem.* **2014**, *750*, 35-40; d) M. C. Joseph, A. J. Swarts, S. F. Mapolie, "Palladium (II) complexes chelated by 1-substituted-4-pyridyl-1H-1,2,3-triazole ligands as catalyst precursors for selective ethylene dimerization", *Appl. Organomet. Chem.* **2020**, *34*, e5595.
- [50] Addition of acid (tosylic) or base (DMAP) resulted in decomposition of the complexes.
- [51] a) R. D. Sommer, A. L. Rheingold, A. J. Goshe, B. Bosnich, "Supramolecular Chemistry: Molecular Recognition and Self-Assembly Using Rigid Spacer-Chelators Bearing

- Cofacial Terpyridyl Palladium(II) Complexes Separated by 7 Å", *J. Am. Chem. Soc.* **2001**, *123*, 3940-3952; b) F. K. Kong, A. K. Chan, M. Ng, K. H. Low, V. W. Yam, "Construction of Discrete Pentanuclear Platinum(II) Stacks with Extended Metal-Metal Interactions by Using Phosphorescent Platinum(II) Tweezers", *Angew. Chem. Int. Ed. Engl.* **2017**, *56*, 15103-15107; c) Y. Yamauchi, M. Yoshizawa, M. Fujita, "Engineering stacks of aromatic rings by the interpenetration of self-assembled coordination cages", *J. Am. Chem. Soc.* **2008**, *130*, 5832-5833; d) T. Murase, K. Otsuka, M. Fujita, "Pairwise selective formation of aromatic stacks in a coordination cage", *J. Am. Chem. Soc.* **2010**, *132*, 7864-7865; e) Y. Yamaki, T. Nakamura, S. Suzuki, M. Yamamura, M. Minoura, T. Nabeshima, "A Self-Assembled Rectangular Host with Terpyridine-Platinum(II) Moieties That Binds Unsubstituted Pentacene in Solution", *Eur. J. Org. Chem.* **2016**, *2016*, 1678-1683.
- [52] a) H. Motschi, C. Nussbaumer, P. S. Pregosin, F. Bachechi, P. Mura, L. Zambonelli, "The trans-Influence in Platinum (II) Complexes. <sup>1</sup>H- and <sup>13</sup>C-NMR. and X-ray structural studies of tridentate Schiff's base complexes of platinum (II)", *Helv. Chim. Acta* **1980**, *63*, 2071-2086; b) A. J. Goshe, J. D. Crowley, B. Bosnich, "Supramolecular recognition: Use of cofacially disposed bis-terpyridyl square-planar complexes in self-assembly and molecular recognition", *Helv. Chim. Acta* **2001**, *84*, 2971-2985.
- [53] The combination of **2Pt** with [Pd<sub>2</sub>L<sub>2</sub>(solvent)<sub>2</sub>]<sup>2+</sup> in [D<sub>3</sub>]acetonitrile resulted in precipitation even at very low equivalencies.
- [54] Screening against 9-methylanthracene and [((E)-2-((2-oxidobenzylidene)amino)-phenolate)(DMSO)platinum(II)] also showed interaction between host and guest.
- [55] www.supramolecular.org.
- [56] a) P. Thordarson, "Determining association constants from titration experiments in supramolecular chemistry", *Chem. Soc. Rev.* **2011**, *40*, 1305-1323; b) F. Ulatowski, K. Dąbrowa, T. Bałakier, J. Jurczak, "Recognizing the Limited Applicability of Job Plots in Studying Host-Guest Interactions in Supramolecular Chemistry", *J. Org. Chem.* **2016**, *81*, 1746-1756.
- [57] a) A. S. Meyer, G. H. Ayres, "The Mole Ratio Method for Spectrophotometric Determination of Complexes in Solution", *J. Am. Chem. Soc.* **1957**, *79*, 49-53; b) D. Brynn Hibbert, P. Thordarson, "The death of the Job plot, transparency, open science and online tools, uncertainty estimation methods and other developments in supramolecular chemistry data analysis", *Chem. Commun.* **2016**, *52*, 12792-12805.
- [58] For example, see; S. Ibanez, E. Peris, "Dimensional Matching versus Induced-Fit Distortions: Binding Affinities of Planar and Curved Polyaromatic Hydrocarbons with a Tetragold Metallorectangle", *Angew. Chem., Int. Ed.* **2020**, *59*, 6860-6865.
- [59] in *Spartan '16*, Wavefunction, Inc., Irvine, CA, **2016**.
- [60] a) M. Käseborn, J. J. Holstein, G. H. Clever, A. Lützen, "A Rotaxane-like Cage-in-Ring Structural Motif for a Metallosupramolecular Pd<sub>6</sub>L<sub>12</sub> Aggregate", *Angew. Chem Int. Ed.* **2018**, *57*, 12171-12175; b) D. Ogata, J. Yuasa, "Dynamic Open Coordination Cage from Nonsymmetrical Imidazole-Pyridine Ditopic Ligands for Turn-On/Off Anion Binding", *Angew. Chem. Int. Ed. Engl.* **2019**, *58*, 18424-18428; c) J. E. M. Lewis, A. Tarzia, A. J. P. White, K. E. Jelfs, "Conformational control of Pd<sub>2</sub>L<sub>4</sub> assemblies with unsymmetrical ligands", *Chem. Sci.* **2020**, *11*, 677-683; d) S. Prusty, K. Yazaki, M. Yoshizawa, D. K. Chand, "A Truncated Molecular Star", *Chem. Eur. J.* **2017**, *23*, 12456-12461; e) S. Samantray, S. Krishnaswamy, D. K. Chand, "Self-assembled conjoined-cages", *Nat. Commun.* **2020**, *11*, 880; f) Y. Tamura, H. Takezawa, M. Fujita, "A Double-Walled Knotted Cage for Guest-Adaptive Molecular Recognition", *J. Am. Chem. Soc.* **2020**, *142*, 5504-5508.
- [61] Allosterism driven by exo-binding of secondary guests has also been used to (non-reversibly) influence encapsulation affinity with retention of core structure, through electrostatic repulsion, see; W. J. Ramsay, J. R. Nitschke, "Two distinct allosteric active sites regulate guest binding within a Fe<sub>8</sub>Mo<sub>12</sub><sup>16+</sup> cubic receptor", *J. Am. Chem. Soc.* **2014**, *136*, 7038-7043.
- [62] V. Martí-Centelles, R. L. Spicer, P. J. Lusby, "Non-covalent allosteric regulation of capsule catalysis", *Chem. Sci.* **2020**, *11*, 3236-3240.